A Structural Integrity Assessment Method for Civil Engineering Structures with a Growing Crack Considering Constraint Effect

Huajing Guo, Wenjie Tang, Kangxin Li, Xiaolong Tong*

***Abstract*—In order to resolve safe running problem of civil engineering structures in process of crack propagation, a constraint-based structural integrity assessment method for civil engineering structures with a growing crack has been developed based on R6 procedure. The equivalence principle of stress intensity factor has been developed to represent influence of crack growth on the structural integrity of cracked structures. The constraint-based *J* integral has been proposed based on the basis of *J*-A_2 solutions. On the basis of option 3 of R6 procedure, the modified failure assessment diagram (FAD) for civil engineering structures with a growing crack has been established considering constraint effect near crack tip and crack growth. Finite element analysis on process of crack propagation of a cracked plate has been performed and the structural integrity has been assessed using modified option 3 of R6 procedure. The results illustrated that high constraint effect could occur near the crack tip of the plate subjected to uniaxial tensile loading, which exhibited significant influence on the *J* integral in the process of crack propagation. The constraint effect and crack growth showed significant influence on the structural integrity of cracked structures, which demonstrated the importance of the newly modified R6 criterion and implied that the integrity assessment results for the structure with a growing crack could be overestimated based on traditional R6 procedure.**

***Index Terms*—integrity assessment, growing crack, constraint effect, modified FAD**

I. Introduction

In practice, crack initiation and propagation could endanger the integrity of civil engineering structures, leading to fracture failure [1-3]. Many efforts have been made on the structural integrity assessment methods to ensure safe running of cracked structures for various industries. Chen et al. [4] studied the difference between the reserve factor in the R6 procedure and the safety coefficient in the single code and established the FAD for the reactor pressure vessel. Han et al. [5] carried out round robin analysis on stress intensity factors to verify the appropriateness of structural integrity assessment methods for austenitic stainless steel pipe welds with circumferential cracks. Kim et al. [6] analyzed the influence of blunt defects on the structural integrity assessment of steels based on a series of tests and finite element simulations. Naib et al. [7] analyzed the suitability of Vickers hardness mapping to provide a weld engineering critical assessment for high strength low alloy steel and suggested an experimental calibration procedure based on weld metal tensile tests. Lei et al. [8] studied the influence of various limit load solutions of the defective elbows on the *J* integrity predictions to support the structural integrity assessment of defective elbows using R6 procedure. Arda et al. [9] developed a shelled UAV system in which structural inspectors were used perform a close visual inspection of the bridge. Guo [10] put forward a multi scale analysis method for crack tip fields considering the influence of micro-cracks has been proposed. Li et al. [11] proposed a data-driven machine learning technique to determine the specific failure assessment curves for full-scale pipeline girth welds based on the resistance tests and finite element analysis. However, the current research was concentrated on the integrity assessment of defective structures with a static crack in which the influence of crack growth was ignored. Therefore, a fitness-for-service procedure is urgent required to assess the structural integrity of civil engineering structures with a growing crack.

Generally, highly constrained specimens with deep cracks are used in fracture toughness testing standards [12-14]. As a result, constraint effect along crack front was used to describe the dependence of fracture toughness on the external factors, such as crack configuration and applied loading, which has extracted much attention from both scholars and engineers. Qian et al. [15] conducted the structural integrity analysis of a cracked reactor pressure vessel subjected to pressurized thermal shocks using K-T approach. Matvienko [16] studied the influence of in-plane and out-of-plane crack tip constraint parameters on plastic zone near the crack tip, the fracture tough-ness and the angle of surface crack growth. Shimodaira et al. [17] investigated the influence of the cladding on the plastic constraint and subsequent evaluation of cracked reactor pressure vessel steel based on three-point bending fracture toughness tests. Zheng et al. [18] investigated the constraint characterization and fracture initiation for actual large scale reactor pressure vessel with semi-elliptical surface cracks based on finite element analysis. Wang et al. [19]

Manuscript received February 14, 2025; revised June 13, 2025.

This work was supported by the National Natural Science Foundation of China (52478312), the Undergraduate Innovative Training Program Project of Hunan Province (S202412658016), the Natural Science Foundation of Hunan Province (2025JJ70290) and Education Department of Hunan Province (24B0616).

Huajing Guo is a lecturer in College of Civil Engineering and Architecture, Hunan Institute of Science and Technology, Yueyang, 414006, China (e-mail: 12020006@hnist.edu.cn).

Wenjie Tang is a graduate student in College of Civil Engineering and Architecture, Hunan Institute of Science and Technology, Yueyang, 414006, China (e-mail: 810229604@qq.com).

Kangxin Li is an undergraduate student in College of Nanhu, Hunan Institute of Science and Technology, Yueyang, 414006, China (e-mail: 3507463588@qq.com).

Xiaolong Tong is a professor in College of Civil Engineering and Architecture, Hunan Institute of Science and Technology, Yueyang, 414006, China (corresponding author to provide phone: +86-0730-8648810; e-mail: 12009016@hnist.edu.cn).

studied the influence of constraint conditions on the reverse plasticity and ratcheting behavior of cracked structures using compact tension test and central-cracked tension tests under cyclic loading condition. However, up to now, the studies on influence of constraint effect on structural integrity were limited to the reactor pressure vessels and there are few studies concentrated on the structural integrity of cracked civil engineering structures considering constraint effect.

Therefore, although many efforts have been made on fracture problem for cracked civil engineering structures, the structural integrity assessment problem of cracked civil engineering structures has not been resolved, especially for the structures with a growing crack. In this paper, a constraint-based structural integrity assessment method for civil engineering structures with a growing crack has been presented based on R6 criterion. The option 3 of R6 criterion has been modified in which constraint-based J integral was proposed considering constraint effect near crack tip. The equivalence principle of stress intensity factor has been developed to establish the FAD for cracked civil engineering structures in the process of crack propagation. Finite element analysis on process of crack propagation of a cracked plate has been performed and the structural integrity has been assessed based on the developed constraint-based assessment method.

II. The Constraint-based Integrity Assessment Method for Structures with a Growing Crack

This section aimed to develop the constraint-based integrity assessment method for civil engineering structures with a growing crack in which three innovative works have been accomplished. Firstly, the equivalence principle of stress intensity factor has been established. Secondly, the constraint-based J integral has been deduced based on J-A_2 solutions. Finally, the FAD for civil engineering structures with a growing crack has been developed considering constraint effect near crack tip and crack length growth.

A. The Equivalence Principle of Stress Intensity Factor

According to fracture mechanics [20], stress intensity factor K is an important fracture parameter to describe the elastic crack tip fields and the K for mode I can be expressed as:

$$K_1 = pY\sqrt{\pi a} \tag{1}$$

where p is applied loading, Y is shape factor, a is half of crack length.

J integral is a path-independent fracture parameter for elastic-plastic crack tip fields and the relationship between K_I and J for elastic problem can be expressed as:

$$J = \frac{1-\nu^2}{E} K_1^2 \tag{2}$$

where E is elastic modulus, ν is Poisson's ratio.

For a given applied loading p_1, shown as figure 1(a), stress intensity factor K_I^1 of the plate with an initial crack length $2a_1$ can be expressed as:

$$K_1^1 = p_1 Y_1 \sqrt{\pi a_1} \tag{3}$$

For an applied loading p_i(i=1, 2, 3, …, nn), shown as figure 1(b), the corresponding stress intensity factor K_I^i of the plate with a growing crack length $2a_i$ can be expressed as:

$$K_1^i = p_i Y_i \sqrt{\pi a_i} \ (i = 1, 2, 3, ..., nn) \tag{4}$$

The solutions of stress intensity factor of cracked structures with different crack length can be equal once the applied loading satisfies the specific requirements, illustrated as figure 1. As a result, the equivalence principle of stress intensity factor can be defined that the solution of stress intensity factor of a structure with an initial crack under a constant applied loading can be equal to that of a growing crack under an effective applied loading. Therefore, the effective applied loading p_{ieff} (i=1, 2, 3, …, nn) can be obtained as:

$$p_{ieff} = p_1 Y_1 / Y_i \sqrt{a_1 / a_i} \quad (i = 1, 2, 3, ..., nn) \tag{5}$$

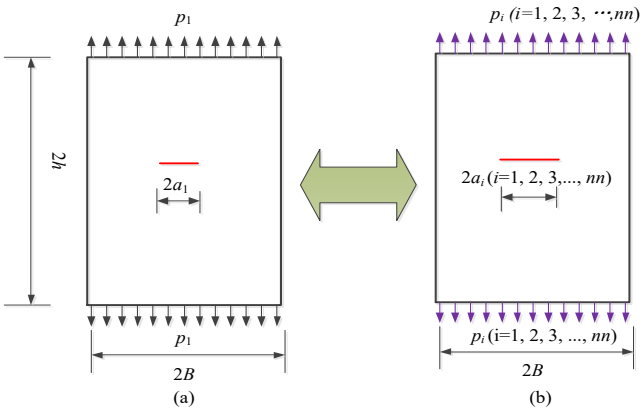

Fig. 1. The equivalence principle of stress intensity factor

B. The Constraint-based J Integral

Constraint effect near crack tip may cause negative consequences to the integrity of cracked structures. Many efforts have been made to represent the influence of constraint effect on fracture behavior of cracked structures. Yang et al. [21] and Chao et al. [22] put forward J-A_2 solutions to describe crack fields in which the constraint effect level was quantified by A_2. The J-A_2 solutions were expressed as:

$$\frac{u_i}{\alpha\varepsilon_s L} = A_1^n \left[\left(\frac{r}{L}\right)^{ns_1+1} \tilde{u}_i^{(1)}(\theta, n) + A_2 \left(\frac{r}{L}\right)^{(n-1)s_1+s_2+1} \tilde{u}_i^{(2)}(\theta, n) + A_2^2 \left(\frac{r}{L}\right)^{(n-1)s_1+s_3+1} \tilde{u}_i^{(3)}(\theta, n) \right] \tag{6-1}$$

$$\frac{\varepsilon_{ij}}{\alpha\varepsilon_s} = A_1^n \left[\left(\frac{r}{L}\right)^{ns_1+1} \tilde{\varepsilon}_{ij}^{(1)}(\theta, n) + A_2 \left(\frac{r}{L}\right)^{(n-1)s_1+s_2+1} \tilde{\varepsilon}_{ij}^{(2)}(\theta, n) + A_2^2 \left(\frac{r}{L}\right)^{(n-1)s_1+s_3+1} \tilde{\varepsilon}_{ij}^{(3)}(\theta, n) \right] \tag{6-2}$$

(6-3)

$$\frac{\sigma_{ij}}{\sigma_s}=A_1\left[\left(\frac{r}{L}\right)^{s1}\tilde{\sigma}_{ij}^{(1)}(\theta,n)+A_2\left(\frac{r}{L}\right)^{s2}\tilde{\sigma}_{ij}^{(2)}(\theta,n)+A_2^2\left(\frac{r}{L}\right)^{s3}\tilde{\sigma}_{ij}^{(3)}(\theta,n)\right]$$

where $\tilde{u}_i(\theta,n)$ is angular displacement, $\tilde{\varepsilon}_{ij}(\theta,n)$ is angular strain, $\tilde{\sigma}_{ij}(\theta,n)$ is angular stress distribution function, r is distance from crack tip, θ is crack angle, σ_{ij} is stress tensor, n is material exponent, L is the characteristic length, A_2 is constraint parameter, s_i (i=1, 2, 3) is the exponent of stress function.

In order to analyze the influence of constraint effect on fracture behavior of cracked civil engineering structures, a constraint-based J_k integral has been deduced to represent the stress field near crack tip based on the equation (6-3):

$$\sigma_{ij}=\sigma_s\left(\frac{J}{\alpha\varepsilon_s\sigma_s Inr}\right)^{-s1}\sigma_s\begin{bmatrix}r^{s1}\tilde{\sigma}_{ij}^{(1)}(\theta,n)+\\A_2r^{s2}\tilde{\sigma}_{ij}^{(2)}(\theta,n)+A_2^2r^{s3}\tilde{\sigma}_{ij}^{(3)}(\theta,n)\end{bmatrix}$$

$$=\left(\frac{\beta J_k}{\alpha\varepsilon_s\sigma_s Inr}\right)^{-s1}\tilde{\sigma}_{ij}^{(1)}(\theta,n) \tag{7}$$

$$s_1=-\frac{1}{n+1} \tag{8}$$

The expression of stress field can be rewritten by substituting the principal stress σ_{yy} into the first term of equation (7):

$$\frac{\sigma_{yy}}{\tilde{\sigma}_{ij}^{(1)}(\theta)+A_2r^{s2-s1}\tilde{\sigma}_{ij}^{(2)}(\theta)+(A_2)^2r^{s3-s1}\tilde{\sigma}_{ij}^{(3)}(\theta)}=\sigma_s\left(\frac{J}{\alpha\varepsilon_s\sigma_s In\,r}\right)^{-s1} \tag{9}$$

Substituting the principal stress σ_{yy} into the second term of equation (7):

$$\frac{\sigma_{yy}}{\tilde{\sigma}_{ij}^{(1)}(\theta)}=\sigma_s\left(\frac{\beta J_k}{\alpha\varepsilon_s\sigma_s Inr}\right)^{-s1} \tag{10}$$

where β is normalized constraint factor for J integral and it is expressed as:

$$\beta=\frac{\left(\frac{\tilde{\sigma}_{ij}^{(1)}(\theta)+A_2r^{s2-s1}\tilde{\sigma}_{ij}^{(2)}(\theta)+(A_2)^2r^{s3-s1}\tilde{\sigma}_{ij}^{(3)}(\theta)}{\tilde{\sigma}_{ij}^{(1)}(\theta)}\right)^{n+1}}{\left(\frac{\tilde{\sigma}_{ij}^{(1)}(\theta)+A_2r^{s2-s1}\tilde{\sigma}_{ij}^{(2)}(\theta)+(A_2)^2r^{s3-s1}\tilde{\sigma}_{ij}^{(3)}(\theta)}{\tilde{\sigma}_{ij}^{(1)}(\theta)}\right)^{n+1}+1} \tag{11}$$

Combining the equations (9) and (10), the constraint-based J_k integral can be obtained:

$$J_k=\frac{J}{\beta}\left(\frac{\tilde{\sigma}_{ij}^{(1)}(\theta)+A_2r^{s2-s1}\tilde{\sigma}_{ij}^{(2)}(\theta)+(A_2)^2r^{s3-s1}\tilde{\sigma}_{ij}^{(3)}(\theta)}{\tilde{\sigma}_{ij}^{(1)}(\theta)}\right)^{n+1} \tag{12}$$

Therefore, the facture failure criterion for elastic-plastic condition can be obtained considering the constraint effect:

$$J_k\le J_C \tag{13}$$

where J_C is elastic-plastic fracture toughness.

C. The Modified R6 Procedure

In practice, the safe running of cracked structures is ensured by structural integrity assessment results using fitness-for-service procedure. R6 two-criterion procedure has been widely used to evaluate the integrity of flawed structures in which FAD is utilized, shown as figure 2.

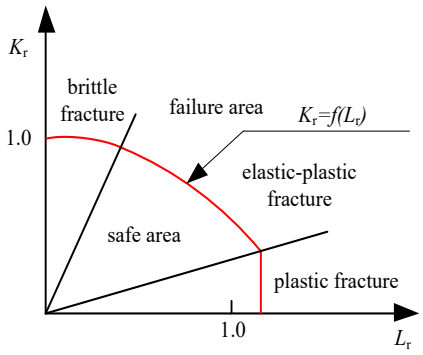

Fig. 2. Schematic diagram of FAD

Three options are available in R6 procedure and the curve of option 3 in FAD is characterized by vertical axis K_r and horizontal axis Lr:

$$L_r=\frac{p}{p_{max}} \tag{14}$$

$$K_r=f_3(L_r)=\sqrt{\frac{J_e}{J}} \tag{15}$$

In the process of crack propagation, the elastic J_e integral and J_e integral should be replaced by $J_e(a, p)$ to investigate the influence of crack length growth. In addition, the J integral should be replaced by the J_K to consider constraint effect near crack tip. As a result, the K_r of option 3 in FAD can be modified as:

$$K_r=f_3(L_r)=\sqrt{\frac{J_e(a,p)}{J_K}} \tag{16}$$

In practice, the influence of crack length on the structural integrity cannot be reflected in the FAD based on traditional R6 procedure. The equivalence principle of stress intensity factor developed in this paper enables to resolve this problem. Submitting equation (5) into equation (14), the Lr of option 3 in FAD can be rewritten as:

$$L_r=\frac{p}{p_{max}}=\frac{p_1Y_1/Y_i\sqrt{a_1/a_i}}{p_1Y_1/Y_{max}\sqrt{a_1/a_{max}}}=\frac{Y_{max}}{Y_i}\sqrt{a_i/a_{max}}\ (i=1,2,3,\ldots,nn) \tag{17}$$

III. The Finite Element Models

Finite element analysis on process of crack propagation of a flawed plate has been performed and the structural integrity has been assessed using modified option 3 of R6 procedure. The plate was made of Q345 steel and the constitutive law of Q345 was represented by Ramberg-Osgood equation:

$$\frac{\varepsilon}{\varepsilon_0}=\frac{\sigma}{\sigma_0}+\alpha\left(\frac{\sigma}{\sigma_0}\right)^n \tag{18}$$

where n is the strain hardening exponent and α is a material constant.

On the basis of the test data of the reference [23], the material parameters were obtained by fitting method, namely n=5 and α=1. In this study, the yield stress σ_s=385MPa, Poisson's ratio ν=0.3 and elastic modulus E=206GPa.

It was assumed that the plate with an initial central crack

a_0=2mm which was subjected to constant uniaxial tensile stress. Four groups of loading were studied in the simulation, namely p_i(i=1, 2, 3, 4)=100MPa, 125MPa, 150MPa and 175MPa. The width 2B and the height 2h of the plate were chosen as 2B=400mm and the height 2h=200mm, shown as figure 1. On the basis of symmetry theory, the one quarter of the plate was simulated. The element type CPS8 was chosen in the simulation and symmetric boundary conditions were applied to the model. To be concise, only the finite element model of the plate with an initial central crack was shown as figure 3. The total number of nodes was 4003 and the total number of units was 1284.

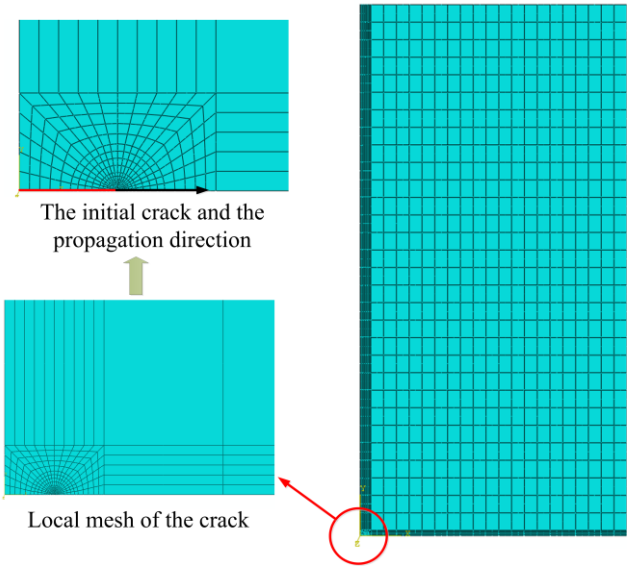

Fig. 3. The finite element model of the plate with an initial central crack

The validity of the finite element models was verified by comparing the theoretical solution of K based on equation (1) with that extracted from finite element numerical results. For the condition where p=100MPa and a_0=2mm, the theoretical solution was K_I=251.3MPa.mm$^{1/2}$ and the corresponding numerical result was K_I=249.7MPa.mm$^{1/2}$. The relative difference between the two results was 0.6%, which demonstrated that the finite element models were reliable.

IV. Finite Element Numerical Results and Discussion

A. Analysis on Constraint Effect near Crack Tip

On the basis of J-A_2 solutions and the numerical results, analysis on constraint effect of the cracked plate in the process of crack propagation under different loading has been performed. In this section, A_2 was used to represent constraint effect and the solution was taken at a normalized distance $r/(J/\sigma_s)$=2-5 from the crack tip. The results were illustrated in figure 4. The conclusions can be drawn based on figure 4:

(1) The value of A_2 exhibited great dependence on crack length growth, which implied that the constraint effect level could be improved in the process of crack propagation.

(2) The value of A_2 increased with increasing of applied loading and normalized distance, which implied that applied loading and normalized distance could enhance the constraint effect near crack tip.

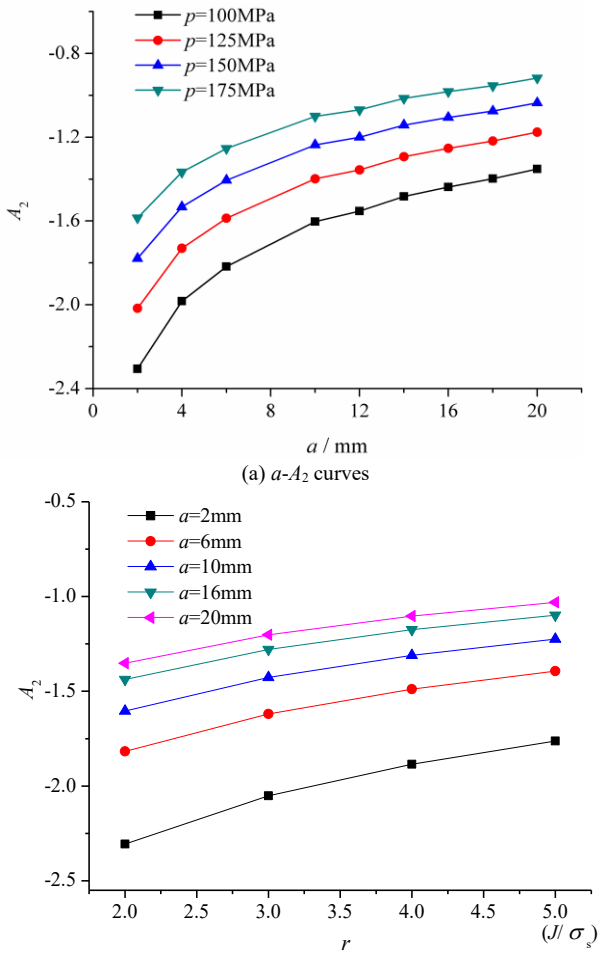

Fig. 4. Constraint variation of the cracked structure

B. The Influence of Constraint Effect on J Integral

In this section, analysis on influence of constraint effect on J integral under different loading condition has been carried out. The values of J integral were directly extracted from the finite element results. On the basis of finite element results, the constraint-based J integral was calculated using equation (12). The results were illustrated in figure 5 and the conclusions can be drawn:

(1) The difference between J integral and constraint-based J integral increased with increase of crack length, which demonstrated that the influence of constraint effect on J integral could become more pronounced in the process of crack propagation.

(2) The increasing of applied loading level could enlarge the difference between J integral and constraint-based J integral.

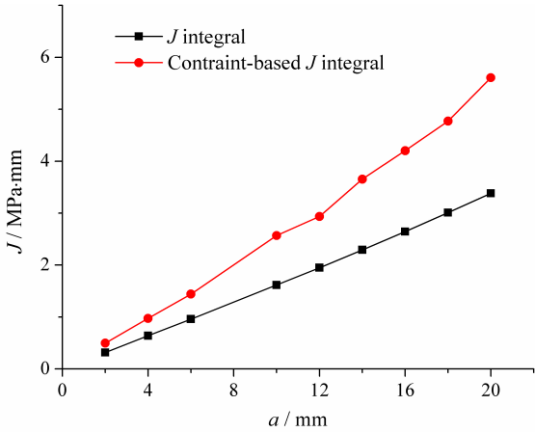

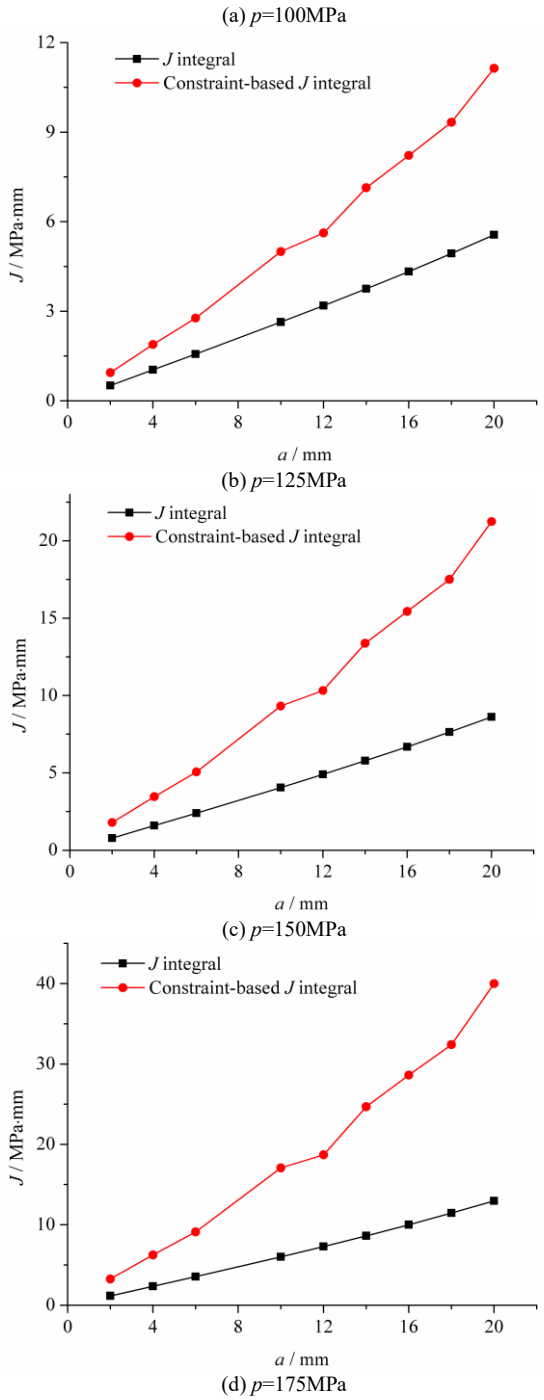

Fig. 5. The distribution of J integral under different loading condition

C. Integrity Assessment for the Cracked Structure in Process of Crack Propagation

In this section, option 3 of R6 procedure and the modified constraint-based R6 procedure were chosen to assess structural integrity of the cracked plate with different crack length. Note that the FAD using option 3 of R6 procedure was expressed by equations (14) and (15) and the FAD using constraint-based R6 procedure was expressed by equations (14) and (16). It was assumed that the plate failed once the crack length reaches the 10% of its width, namely the a_{max}=20mm. Based on the finite element numerical results, integrity assessment curves of the structure with different crack length have been provided using the two methods and comparison between the two kinds of assessment results has been made, shown as figure 6 and figure 7.

In practice, civil engineering structures usually are subjected to a constant loading and crack growth could endanger integrity of cracked structures. However, the assessment results based on R6 procedure were incapable of describing the influence of crack growth. Therefore, structural integrity assessment for the flawed structure with a growing crack length has been performed using the modified R6 procedure in which the newly developed FAD was expressed by equations (16) and (17), shown as figure 8.

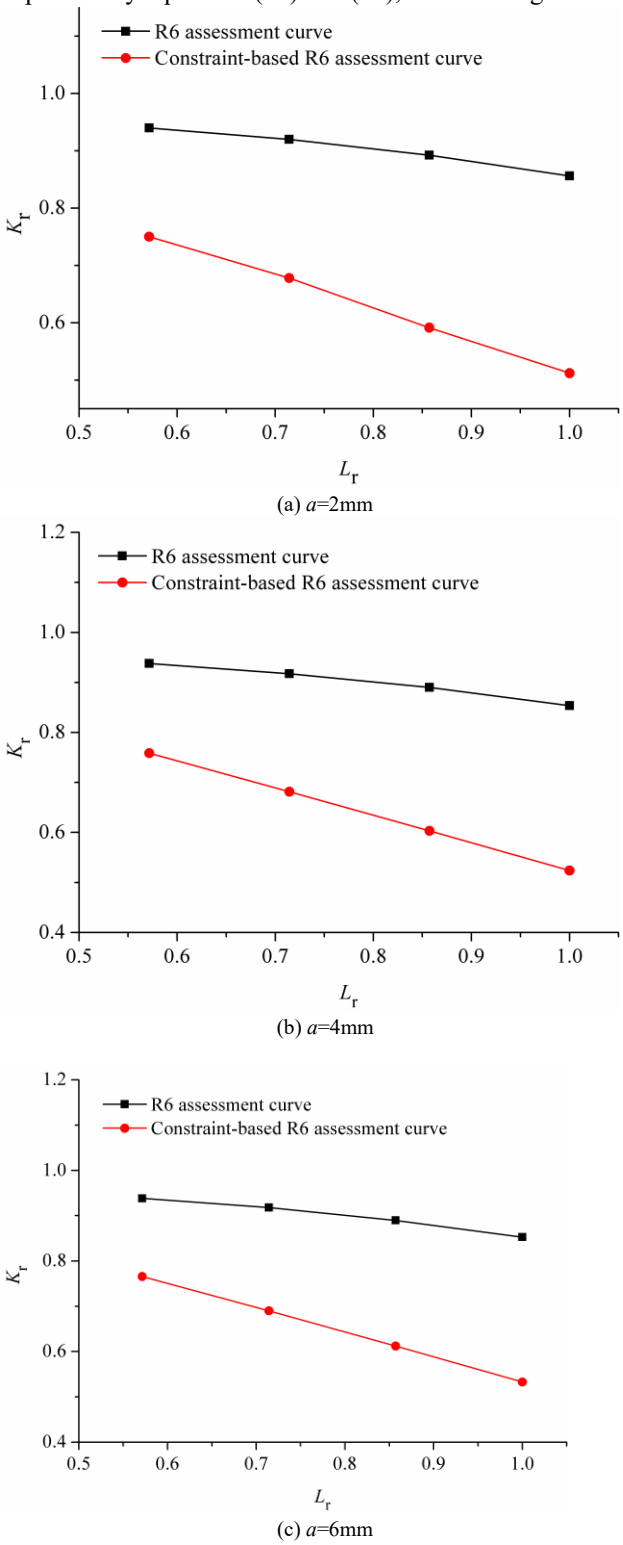

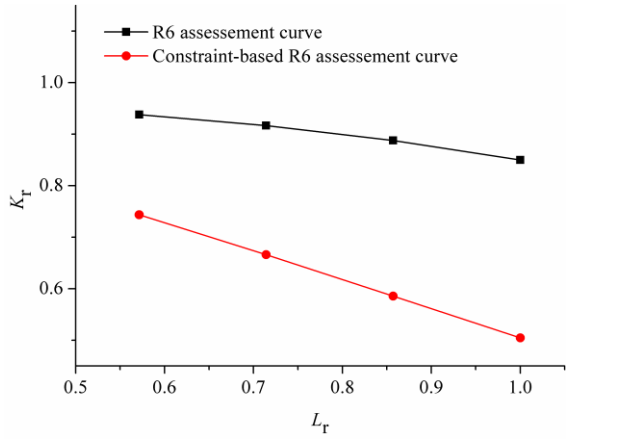

(d) a=10mm

Fig. 6. Integrity assessment curves of the structure with relatively short crack length

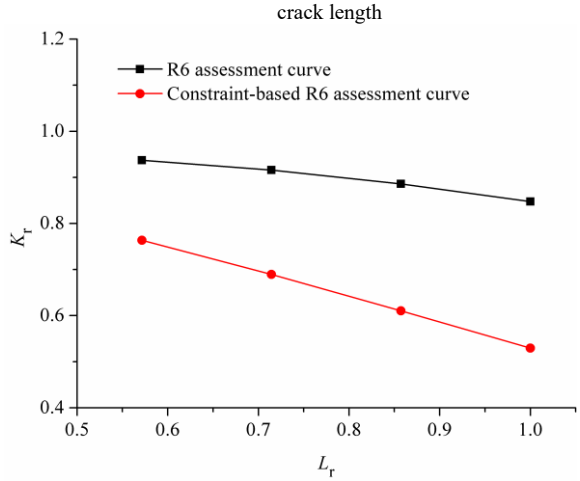

(a) a=12mm

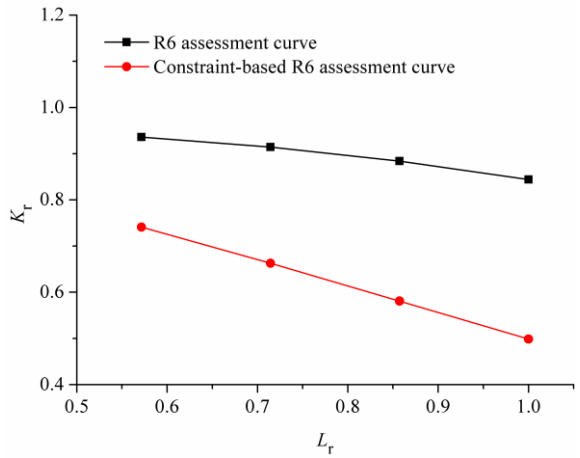

(b) a=14mm

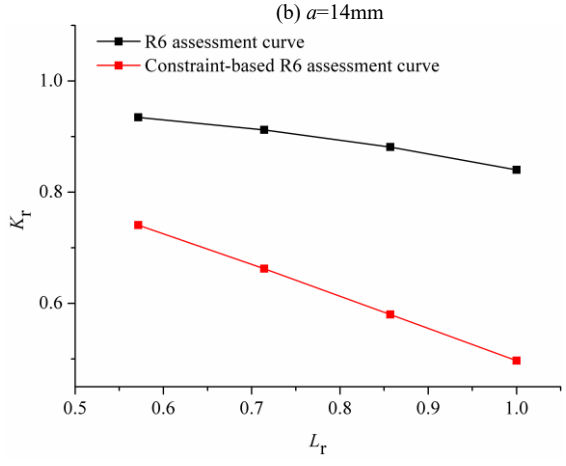

(c) a=16mm

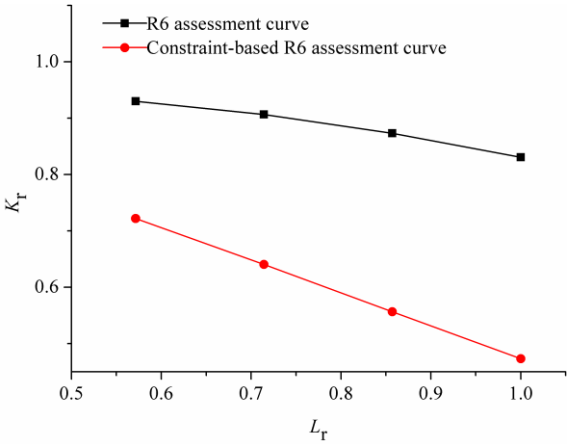

(d) a=20mm

Fig. 7. Integrity assessment curves of the structure with relatively long crack length

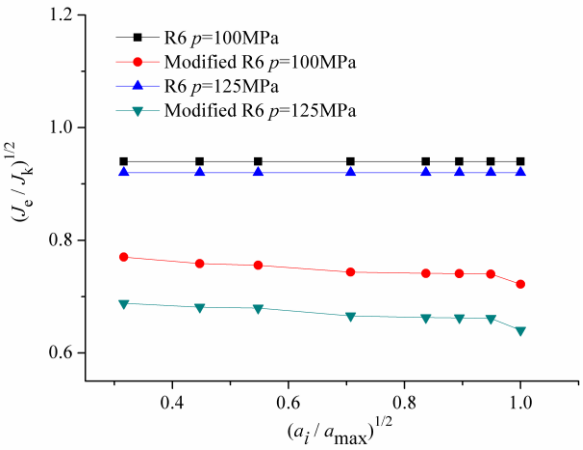

(a) p=100MPa and p=125MPa

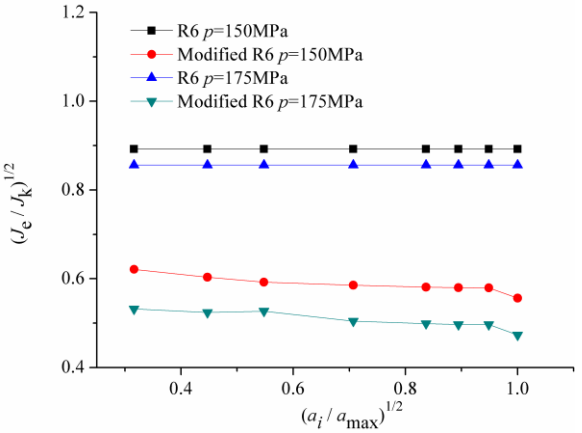

(b) p=150MPa and p=175MPa

Fig.8. Integrity assessment curves of the structure with a growing crack

The conclusions can be drawn from figures 6-8:

(1) The safe area in FAD based on constraint-based R6 procedure was much smaller than that based on R6 procedure, which implied that constraint effect could markedly endanger integrity of cracked structures.

(2) The influence of constraint effect and crack length growth on the structural integrity of cracked structures in the process of crack propagation can be presented in the newly established FAD using modified R6 criterion.

(3) The safe area in FAD based on modified R6 procedure gradually decreased in process of crack propagation, which implied that the integrity assessment results based on traditional R6 procedure for the structure with a growing crack may be overestimated.

V. Conclusions

In order to resolve safe running problem of cracked civil engineering structures in process of crack propagation, a constraint-based structural integrity assessment method for civil engineering structures with a growing crack has been developed based on R6 criterion. Finite element analysis on process of crack propagation of a cracked plate has been performed and the structural integrity has been assessed using modified option 3 of R6 criterion. The main works and conclusions were briefly summarized as following:

(1) The equivalence principle of stress intensity factor for structures with different crack length has been put forward in which the effective applied loading was derived.

(2) A modified FAD for cracked civil engineering structures with a growing crack has been established in which a constraint-based *J* integral was proposed.

(3) High constraint effect could occur near the crack tip of the plate subjected to tensile loading, which exhibited significant influence on the *J* integral in the process of crack propagation.

(4) The constraint effect and crack growth showed significant influence on the structural integrity of cracked structures, which implied that the integrity assessment results for the structure with a growing crack could be overestimated based on traditional R6 procedure.

Furthermore, it is significant to apply the numerical results and theorical conclusions to real-world solutions. In this study, the newly developed equivalence principle of stress intensity factor and the modified constraint-based J integral enable to resolve the fracture failure problems for the cracked structures in the process of crack propagation to some degree, which also support the development of fracture mechanics discipline. In addition, R6 two-criterion procedure is a fitness-for-service method which has been widely used to assess structural integrity of flawed structures using FAD. This study proposed an innovative method to guarantee the safe running by establishing a new FAD for cracked structures with a growing crack.

References

[1] S. Bin, T. Guo, "A multi-scale model from microscopic cracks to macroscopic damage of concrete at elevated temperatures," Int. J. Damage Mech. vol. 33, no.3, pp. 177-192, 2024.

[2] Y.W. Liu, S. Bin, T. Guo, Z.X. Li, "Multiscale damage analysis of engineering structures from material level to structural level: a systematic review," Int. J. Struct. Integr. vol. 16, no.2, pp. pp. 275-310, 2025.

[3] J. Xu, L. Ma, X.C. Xiao, J.X. Jin, C.Y. Meng, "The influence of defect shape on the cracking behavior of brittle materials," J. Build. Eng. vol. 79, pp.107805, 2023.

[4] M.Y. Chen, F. Lu, R.S. Wang, "Use of the failure assessment diagram to evaluate the safety of the reactor pressure vessel," J. Press. Vess T.-ASME. vol. 137, no. 5, pp. 051203, 2015.

[5] C.G. Han, Y.S. Chang, J.S. Kim, M.W. Kim, "Round robin analyses on stress intensity factors of inner surface cracks in welded stainless steel pipes," Nucl. Eng. Technol. vol. 48, no. 6, pp. 1412-1422, 2016.

[6] J.S. Kim, N.O. Larrosa, A.J. Horn, Y.J. Kim, R.A. Ainsworth, "Notch bluntness effects on fracture toughness of a modified S690 steel at 150℃," Eng. Fract. Mech. vol. 188, pp. 250-267, 2018.

[7] S. Naib, W. De Waele, P. Stefane, N. Gubeljak, S. Hertelé, "Crack driving force prediction in heterogeneous welds using Vickers hardness maps and hardness transfer functions," Eng. Fract. Mech. vol. 201, pp. 322-335, 2018.

[8] Y.B. Lei, P. Budden, "J predictions for defective pipe elbows via the reference stress method," J. Press. Vess T.-ASME. vol. 144, no. 3, pp. 031303, 2022.

[9] M. Arda, J. Pao, C.J. Salaan, et al. "Shelled unmanned aerial system for bridge structural health monitoring," Engineering Letters, vol. 31, no. 4, pp. 1415-1433, 2023.

[10] H.J. Guo, "Analysis on the fracture mechanism of cracked materials considering the influence of micro-cracks in the vicinity of the macro-crack tip," IAENG International Journal of Applied Mathematics, vol. 53, no. 1, pp. 225-230, 2023.

[11] S.Y. Li, B.M. Gong, L.S. Dai, C.Y. Deng, X.J. Di, "Data-driven probabilistic failure assessment curve based on similitude principle," Int. J. Solids Struct. vol. 295, pp. 112819. 2024.

[12] K. Wallin, "Quantifying T stress controlled constraint by the master curve transition temperature T0," Eng. Fract. Mech. vol. 68, pp. 303-328, 2001.

[13] X.K. Zhu, J.A. Joyce, "Review of fracture toughness (G, K, J, CTOD, CTOA) testing and standardization," Eng. Fract. Mech. vol. 85, pp. 1-46, 2012.

[14] J.S. Kim, J.M. Seo, J.Y. Kang, Y.Y. Jang, Y.J. Lee, K.W. Kim, "Constraint-corrected fracture mechanics analysis of nozzle crotch corners in pressurized water reactors," Nucl. Eng. Technol. vol. 54, no. 5, pp. 1726-1746, 2022.

[15] G. Qian, M. Niffenegger, "Integrity analysis of a reactor pressure vessel subjected to pressurized thermal shocks by considering constraint effect," Eng. Fract. Mech. vol. 112, pp. 14-25, 2013.

[16] Y.G. Matvienko, "The effect of crack-tip constraint in some problems of fracture mechanics," Eng. Fail. Anal. vol. 110, pp. 104413, 2020.

[17] M. Shimodaira, T. Tobita, H. Takamizawa, J. Katsuyama, S. Hanawa, "Constraint effect on fracture behavior of underclad crack in reactor pressure vessel," J. Press. Vess-T.-ASME. vol. 144, no. 1, pp. 011304, 2022.

[18] Y. Zheng, G.Z. Wang, S.T. Tu, F.Z. Xuan, "Constraint characterization and fracture initiation analysis for semi-elliptical surface cracks in reactor pressure vessel," Int. J. Pres. Ves. Pip. vol. 202, pp. 104910, 2023.

[19] X.X. Wang, J. Yang, H.F. Chen, Z.Y. Ma, F.Z. Xuan, "Effect of constraint on cyclic plastic behaviours of cracked bodies and the establishment of unified constraint correlation," Eur. J. Mech. A-Solid. Vol. 97, pp. 104857, 2023.

[20] J.J. Lewandowski, "Modern fracture mechanics," Philos. Mag. vol. 93, no. 28-30, pp. 3893-3906, 2013.

[21] S. Yang, Y.J. Chao, M.A. Sutton, "Higher order asymptotic crack tip fields in a power-law hardening material," Eng. Fract. Mech. vol. 45, pp. 1-20, 1993.

[22] Y.J. Chao, S. Yang, M.A. Sutton, "On the fracture of solids characterized by one or two parameters: theory and practice," J. Mech. Phys. Solids. vol. 42, pp. 629–64, 1994.

[23] Y.R. Luo, Q.Y. Wang, Y.L. Liu, C.X. Huang, "Low cycle fatigue properties of steel structure materials Q235 and Q345," Journal of Sichuan University (Engineering Science Edition). vol. 44, no. 2, pp. 169-175, 2012.